



## Detailed Analysis of IMPATT-Diode Loaded Active Rectangular Patch Microstrip Antenna

Arvind Mishra<sup>1</sup>, Km Pankaj<sup>2</sup>, B P Singh<sup>3</sup>

<sup>1</sup>Department of Physics, G L Bajaj Institute of Technologys and Management, Greater Noida, (India)

<sup>2</sup>Department of Physics, Noida Institute of Engineering and Technology, Greater Noida, (India)

<sup>3</sup>Department of Physics, Institute of Basic Sciences, Dr B R Ambedekar University, Agra,(India)

### ABSTRACT

The present work describes the circuit model based detailed analysis of symmetrically IMPATT diode loaded microstrip antenna at extremely high frequency range (EHF). To optimize the antenna characteristics, a systematic study on various parameters viz. resonant frequency, input impedance, voltage standing wave ratio (VSWR), return loss, band width, radiation pattern etc. has been carried out as a function of IMPATT diode bias voltage. The study reveals that the IMPATT-integrated patch offers wide tenability, better matching, and enhanced radiated power as compared to the patch alone. The maximum frequency agility is found to be of 614 MHz. It has also been noted that the active diode loaded patch radiations are more powerful i.e. 0.19 dB as compared to single patch design. Thus the IMPATT-diode integrated patch can be used to achieve the electronic frequency tuning and the power tuning with bias voltage.

### I. INTRODUCTION

Recent research into quasi-optical power combining has centered on using large active microwave solid state devices providing localized power derive from microstrip patch antenna elements. These techniques allow monolithic implementation by fabricating both active devices and antenna on a single semiconductor substrate. The circuit can be made at low cost and should have many applications in radar communication, high speed vehicles and EW systems. For power combining and active array applications, considerable success has been achieved by using MESFET, Tunnel diode operated etc. with the microstrip patch antenna with a view to improving the antenna performance[1-4]. However, little efforts have been made to predict the performance of IMPATT-diode integrated microstrip antenna [5]. The major advantage of using an IMPATT-diode is its capability of producing higher frequencies and power than other two terminal microwave solid state devices. In the present endeavor IMPATT-diode integrated patch is studied theoretically in the millimeter range of frequency. Further the results obtained from entire investigation are also compared with rectangular patch only.

### II. THEORETICAL CONSIDERATION

The structure of the antenna integrated with IMPATT-diode is shown in f Fig. 1(a,b). The patch is feed through a coaxial line at distance  $x_0$  from the radiating edge. The IMPATT-diode employs impact-ionization and transit time properties of semiconductor structures to produce negative resistance properties of semiconductor at microwave frequencies. Owing to the negative resistance properties, it can be used as an oscillator. The IMPATT-

diode is mounted between the patch and the ground plane and biasing is effected by applying DC voltage to the patch and plane. The equivalent circuit consisting of a parallel combination of resistance ( $R$ ), inductance ( $L$ ) and capacitance ( $C$ ) is shown in Fig. 1(c). According to modal expansion cavity model, the values  $R, L$  and  $C$  are given by[6]

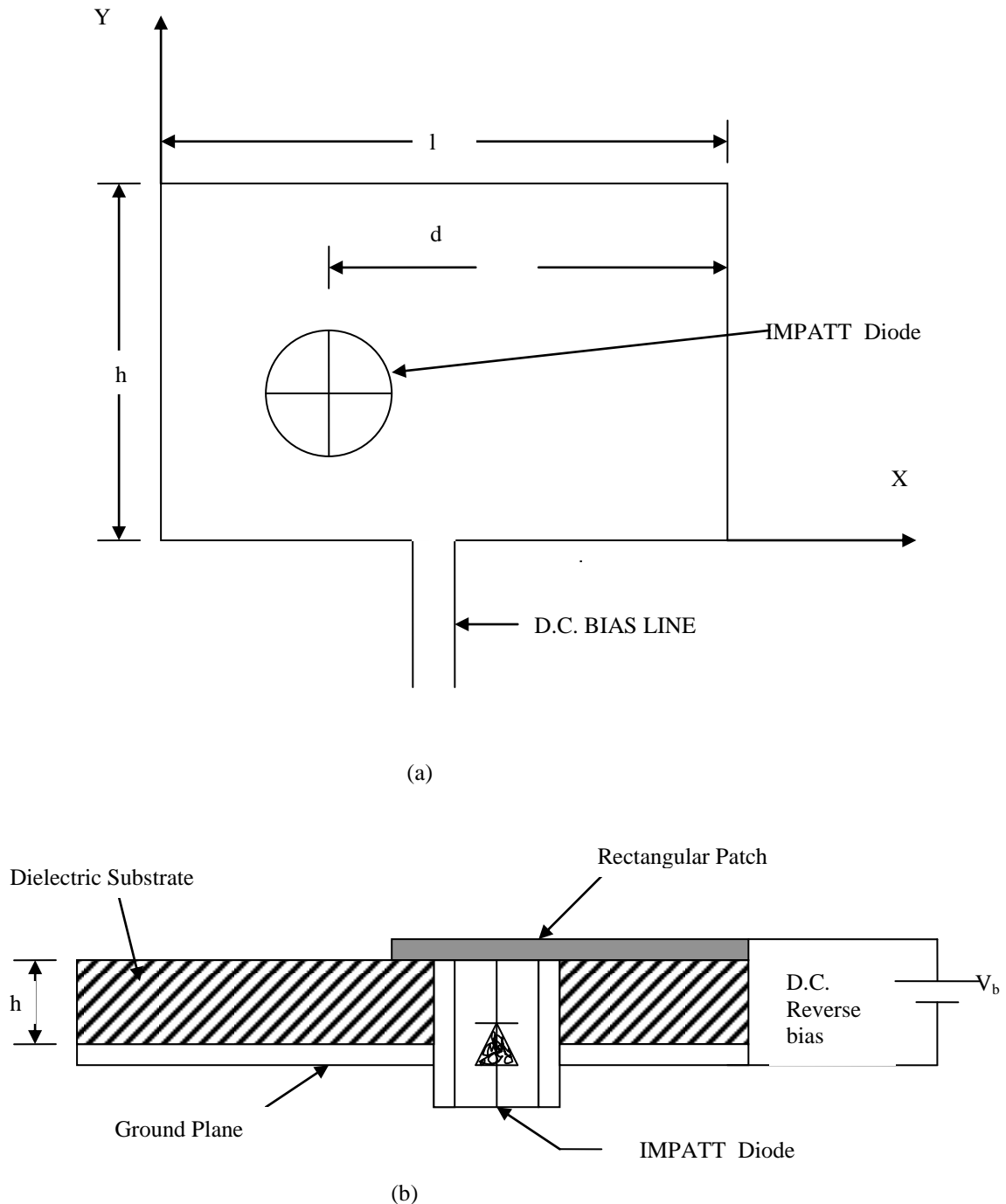


**Fig.1:** (a) Top view of IMPATT integrated microstrip patch with location of diode placement and  
(b) Side view of IMPATT integrated patch antenna.

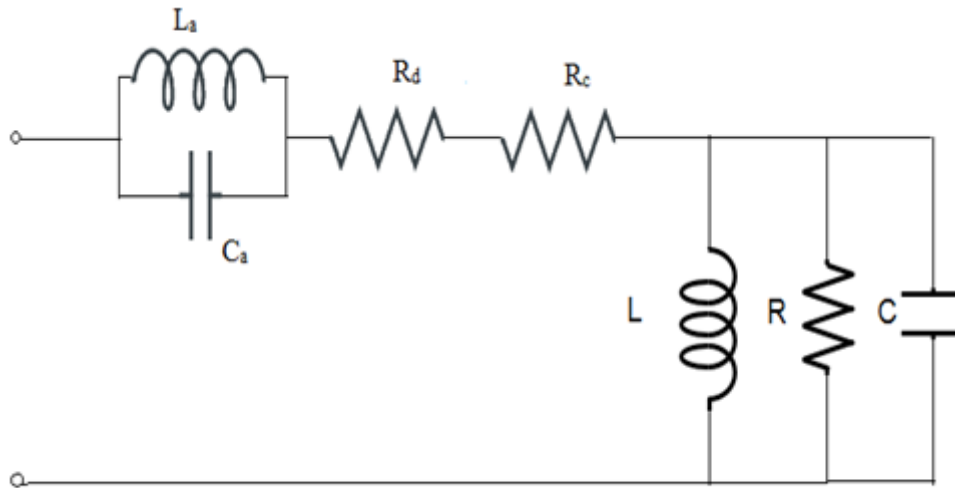


**Fig.1(c): Equivalent circuit of IMPATT diode integrated patch**

$$C = \frac{\epsilon_0 \epsilon_r}{2h} \cos^{-2} \left( \frac{\pi x_0}{l} \right) \quad (1)$$

$$L = \lim_{\omega \rightarrow \infty} \frac{x_{10}}{j\omega} = \frac{1}{C\omega_0^2} \quad (2)$$

and

$$R = \frac{Q_r}{\omega_r C} \quad (3)$$

where  $Q_r$  is the radiation quality factor given by

$$Q_r = \frac{c\sqrt{\omega_{eff}}}{4hf_r} \quad (4)$$

Here  $c$  is the velocity of light,  $\omega_r = 2\pi f_r$ ,  $f_r$  being the resonant frequency,  $x_0$  is the  $x$ -coordinate of the feed point,  $\omega_{eff}$  is the effective permittivity of the medium and is given by

$$\omega_{eff} = \frac{1}{2} \left[ (\epsilon_r + 1) + (\epsilon_r - 1) \left( 1 + \frac{10h}{w} \right)^{-\frac{1}{2}} \right] \quad (5)$$

Where  $\epsilon_r$  is the relative permittivity of the substrate material,  $l$  is the length of the the patch,  $w$  is the width of the patch, and  $h$  is the thickness of the substrate. In millimeter wave range, the calculation for length and width are done according to the moment method solution of the printed rectangular radiating element on a grounded dielectric slab[7].

The input impedance of rectangular patch equivalent to  $R - L - C$  network, shown in the Fig. 1(c) is calculated as

$$Z_{in} = \frac{R\omega^2 L^2 + jR^2(\omega L - \omega^2 L^2 C)}{R^2(1 - \omega^2 LC) + \omega^2 L^2} \quad (6)$$

Separating for real and imaginary parts, we get

$$R_e[Z_{in}] = \frac{R\omega^2 L^2}{R^2(1 - \omega^2 LC)^2 + \omega^2 L^2} \quad (7)$$

$$I_m[Z_{in}] = \frac{R^2(\omega L - \omega^3 L^2 C)}{R^2(1 - \omega^2 LC)^2 + \omega^2 L^2} \quad (8)$$

Impedance of the tank circuit containing avalanche inductance ( $L_a$ ) and capacitance ( $C_a$ ) is

$$Z_1 = \frac{j\omega L_a}{(1 - \omega^2 L_a C_a)}$$

and the impedance contribution of resistors ( $R_s$ ) and ( $R_d$ ) to the total impedance of the circuit is  $Z_2 = R_s + R_d$

Therefore the total impedance of the active patch circuit is given by

$$Z = Z_{in} + Z_1 + Z_2 =$$

$$\left[ R_d + R_s + \frac{R\omega^2 L^2}{R^2(1-\omega^2 LC)2+\omega^2 L^2} \right] + j\omega \left[ \frac{L_a}{(1-\omega^2 L_a C_a)} + \frac{R^2 L(1-\omega^2 LC)}{R^2(1-\omega^2 LC)2+\omega^2 L^2} \right] \quad (9)$$

Separating for real and imaginary parts,

$$R_e[Z] = \left[ R_d + R_s + \frac{R\omega^2 L^2}{R^2(1-\omega^2 LC)2+\omega^2 L^2} \right] \quad (10)$$

$$I_m[Z] = \left[ \frac{L_a}{(1-\omega^2 L_a C_a)} + \frac{R^2 L(1-\omega^2 LC)}{R^2(1-\omega^2 LC)2+\omega^2 L^2} \right] \quad (11)$$

In order to evaluate the effected resonance frequency of the active patch, the imaginary part of the input impedance,  $I_m[Z]$  is evaluated to zero, i.e.

$$\frac{L_a}{(1-\omega^2 L_a C_a)} + \frac{R^2 L(1-\omega^2 LC)}{R^2(1-\omega^2 LC)2+\omega^2 L^2} = 0$$

$$L_a[R^2(1-\omega^2 LC)2+\omega^2 L^2] + (1-\omega^2 L_a C_a)R^2 L(1-\omega^2 LC) = 0$$

$$\omega^4(R^2 L^2 C^2 L_a + R^2 L^2 C L_a C_a) + \omega^2(L^2 L_a - 2R^2 L C L_a - R^2 L L_a C_a - R^2 L^2 C) + R^2 L + R^2 L_a = 0$$

$$\omega^4 R^2 L^2 C L_a (C + C_a) - \omega^2 [R^2 L^2 C + R^2 L L_a (2C + C_a) - L^2 L_a] + R^2 (L + L_a) = 0$$

which is quadratic equation of  $\omega^2$  having the roots

$$\omega_r^2 = \frac{1}{2R^2 L^2 C L_a (C + C_a)} [R^2 L^2 C + R^2 L L_a (2C + C_a) - L^2 L_a] \pm \sqrt{[R^2 L^2 C + R^2 L L_a (2C + C_a) - L^2 L_a]^2 - 4R^2 L^2 C L_a (C + C_a) R^2 (L + L_a)}$$

which gives

$$\omega_r = \sqrt{\frac{P \pm Q}{2M}} \quad (12)$$

where

$$P = R^2 L^2 C + R^2 L L_a (2C + C_a) - L^2 L_a$$

$$Q = \{[R^2 L^2 C + R^2 L L_a (2C + C_a) - L^2 L_a]^2 - 4R^2 L^2 C L_a (C + C_a) R^2 (L + L_a)\}^{1/2}$$

$$M = R^2 L^2 C L_a (C + C_a)$$

Therefore, the resonance frequency ( $f_r$ ) is written as

$$f_r = \frac{\omega_r}{2\pi} = \frac{1}{2\pi} \left[ \frac{P \pm Q}{2M} \right]^{1/2} \quad (13)$$

The maximum voltage that can be applied across the diode is given by [8]

$$V = \int_0^{X_d} E \cdot dx \quad (14)$$

where  $X_d$  is the depletion length and  $E$  is the electric field. This maximum applied voltage is limited by the breakdown voltage. Furthermore, the maximum current that can be carried by the diode is also limited by the avalanche breakdown process, for the current in the space-charge region causes an increase in the electric field.

The maximum current is given by

$$I = J \cdot A = \sigma \cdot E \cdot A = \frac{\epsilon_s}{\tau} \cdot E \cdot A = \frac{V_d \epsilon_s E A}{X_d} = \frac{V_d \epsilon_s V A}{X_d^2} \quad (15)$$

where  $A$  is the diode cross-section area and  $\tau$  is the transit time.



The IMPATT diode mainly consists of three regions namely, avalanche region, drift region and inactive region. The avalanche region behaves as an inductance-capacitance circuit, where the inductance ( $L_a$ ) and capacitance ( $C_a$ ) vary with respect to current and width of the avalanche region respectively, they are given as [9]

$$L_a = \frac{X_a}{2I\alpha v_d} \quad (16)$$

And

$$C_a = \frac{\epsilon_s A}{X_a} \quad (17)$$

where  $X_a$  is the width of an avalanche region,  $\epsilon_s$  is the semiconductor permittivity, A is the diode cross-section area and  $\alpha$  is the derivative of ionization coefficient with electric field.

The bandwidth is mathematically defined as

$$BW = \frac{S-1}{Q_T \sqrt{S}} \quad (18)$$

where S is the VSWR and  $Q_T$  is the total quality factor.

The theoretical E-plane radiation pattern for the microstrip patch can be calculated using the following relation [10]

$$E_\theta = \frac{-jV_0 k_0 w e^{-jk_0 r}}{\pi r} \cos(kh \cos\theta) \cdot \frac{\sin\left(\left(\frac{k_0 w}{2}\right) \sin\theta \sin\phi\right)}{\left(\frac{k_0 w}{2}\right) \sin\theta \sin\phi} \cos\left\{\left(\frac{k_0 l}{2}\right) \sin\theta \sin\phi\right\} \cos\phi \quad (19)$$

for  $0 \leq \phi \leq \pi/2$

and

$$E_\phi = E_\theta \cos\theta \sin\phi \quad \text{for } 0 \leq \phi \leq \pi/2 \quad (20)$$

where  $V_0$  is the radiation edge voltage, r be the distance of any arbitrary point and k be the constant given by

$$k = k_0 \sqrt{\epsilon_r} = \frac{2\pi}{\lambda_0} \sqrt{\epsilon_r}$$

Besides these parameters some other viz. VSWR, mismatch loss, reflection coefficient and return loss are calculated at different reverse bias voltage.

### III. DESIGN DETAILS

The IMPATT-diode loaded rectangular microstrip antenna is designed using various parameters of rectangular microstrip antenna and IMATT-diode, the details of which are given in Tables 1 and 2.

### IV. DISCUSSION OF RESULTS

The variation of resonant frequency of IMPATT-loaded patch with reverse bias voltage is shown in Fig.2. From this figure it is noted that resonant frequency increases almost linearly with reverse bias voltage. This increment in resonant frequency is higher at lower reverse bias voltage (up to 60V). When reverse bias voltage is further increased, the increment of resonant frequency lightly reduces and gains almost a constant value beyond 75 V, which is in accordance with the fact that increasing bias voltage, increases the current in device resulting in enhancement in the resonance frequency. The range of frequency obtainable for operation is 613.5 MHz and the antenna could be operated in the millimeter wave range (34.105 – 34.719 GHz). It is evidently clear that the IMPATT-loaded patch can be operated with varying tenability at millimeter wave range by controlling the bias

voltage of suitable device integrated with the patch. The behavior of impedance (real, imaginary and effective) as a function of bias voltage is shown in Fig.3.

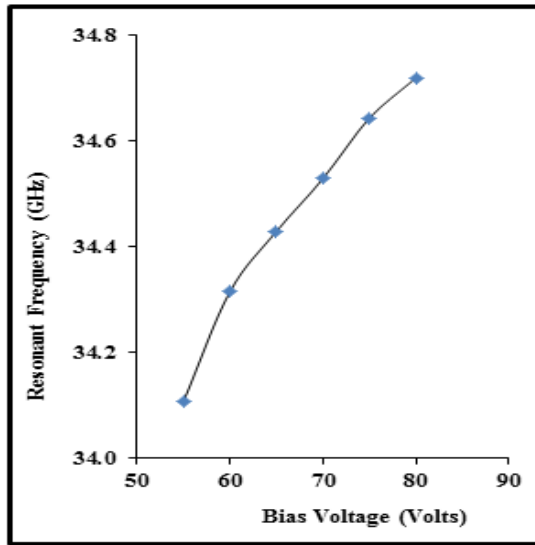


Fig. 2: Variation of resonant frequency versus bias voltage for IMPATT diode loaded RMSA.

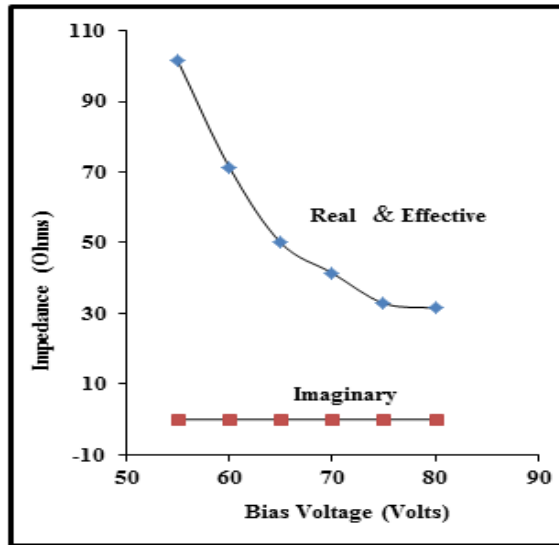


Fig. 3: Variation of Impedance versus bias voltage for IMPATT diode loaded RMSA.

From these plots it is observed that the real part of impedance  $R_e [Z]$  with increasing bias voltage in which the decrement is comparatively less at high values of bias voltages. The examination of imaginary part of impedance  $I_m [Z]$  of IMPATT-loaded patch indicate that it behaves as almost resistive network for the entire range of operation and the circuit may resonate at any bias voltage. This further reveals that such an antenna may work satisfactorily for the feed impedance ranging from 31.53 – 101.54 ohms.

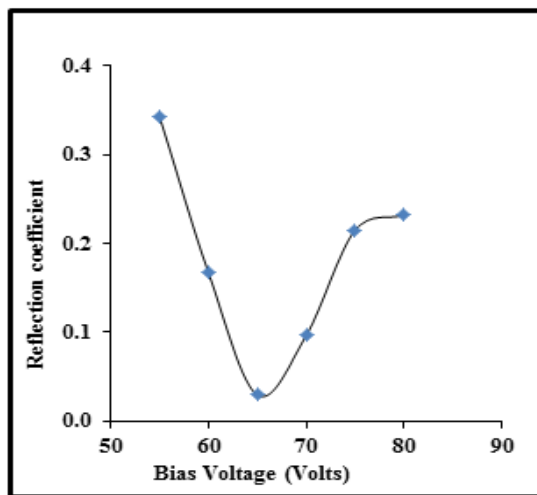


Fig. 4: Variation of reflection coefficient versus bias voltage for IMPATT diode loaded RMSA.

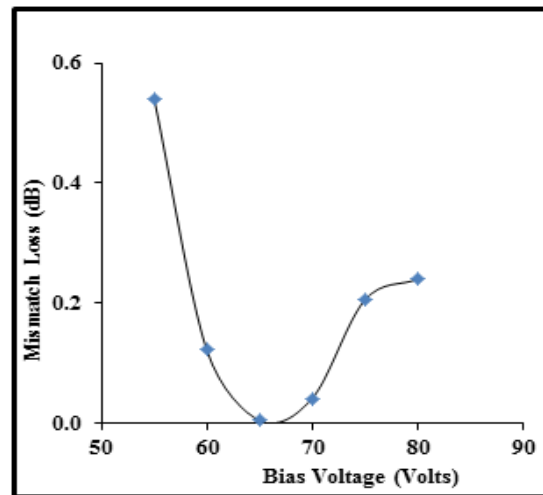
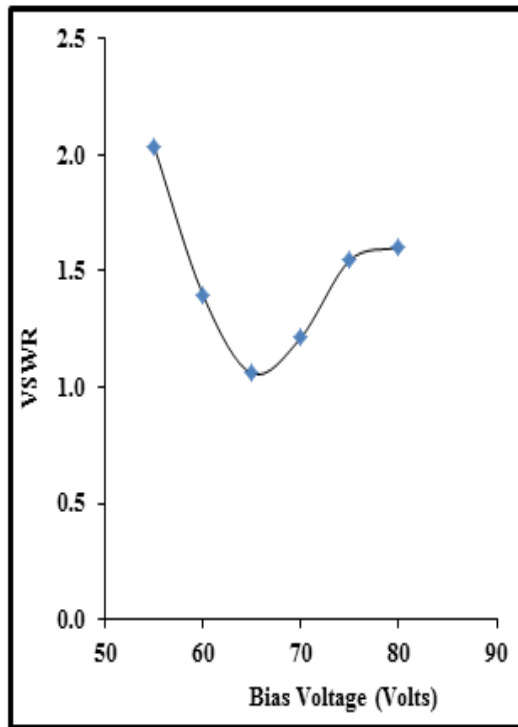


Fig. 5: Variation of mismatch loss versus bias voltage for IMPATT diode loaded RMSA.

The reflection coefficient ( $\rho$ ) plot for IMPATT-diode loaded patch is shown in Fig.4 for different bias voltage. The reflection coefficient for the proposed antenna gets the highest value at lower bias voltage which rapidly decrease to a lowest value and thereafter with the increase of reverse bias voltage reflection coefficient is further increased. The results obtained from reflection coefficient plots are further corroborated from the mismatch loss data shown in Fig.5. The results obtained from these curves are justified due to the fact that the antenna is connected to the 50 ohm feed line and the real part of the input impedance at 65 V shows the value near 50, giving

the best matching of the device. This ensures the satisfactory operation of the antenna for the entire range without any power loss.



**Fig.6: Variation of VSWR versus bias voltage for IMPATT diode loaded RMSA.**

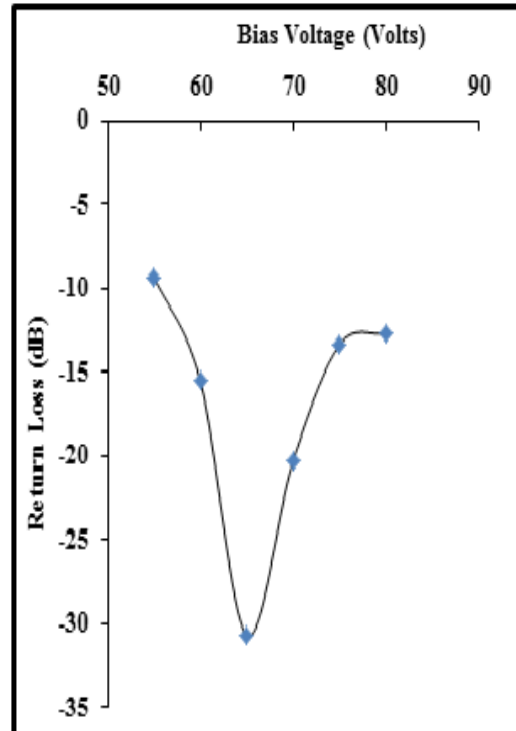


**Fig.7: Variation of return loss versus bias voltage for IMPATT diode loaded RMSA.**

The variation of input VSWR with reverse bias voltage (Fig.6) for IMPATT diode-loaded patch again justifies the above results as the patch antenna exhibits lowest value of VSWR (1.06: 1) at reverse bias voltage of 65 V. The improvement in the VSWR within bias range 50 – 80 V is attributed to the fact that the  $|Z|$  shows the decreasing nature in the same bias range, which shifted the proposed antenna away from the best matching condition. The variation of return loss with bias voltage is shown in Fig.7. It is observed that the minimum of the return loss changes to higher bias voltage for the case of IMPATT diode –loaded patch antenna and the value of return loss remains within acceptable limits. This shows that the antenna can be operated for the entire range of bias voltage without any significant change in the performance of the antenna. The variation of band-width with reverse bias voltage is shown in Fig.8 for the two values of VSWR (1.5:1 and 2:1). It is observed that the antenna maintains almost a constant value with the reverse bias voltage for both the cases. However, for the case 2:1 VSWR, there is sudden decrement in band-width beyond 70 V which improves after 75 V and again maintain the same value at 80 V, which is in accordance with the fact that at higher VSWR as impedance decreases from its matching value, the power loss increases which makes the band-width undisciplined. This unwanted behavior is further catalyzed by inherent noise of semiconductor diode at high resonant frequencies. This is justified because the total quality factor of the antenna does not vary significantly with reverse bias voltage (Fig.9). Further the value of quality factor is very low. Since the band-width is inversely proportional to quality factor, the low value of quality factor makes the band-width of IMPATT diode-loaded patch quite high. Typically the band-width is around 20% for VSWR 1.5:1 and around 35% for VSWR 2:1.

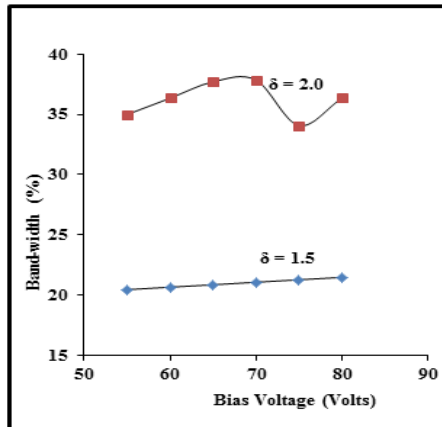


Fig.8: Variation of band-width versus bias voltage for IMPATT diode loaded RMSA.

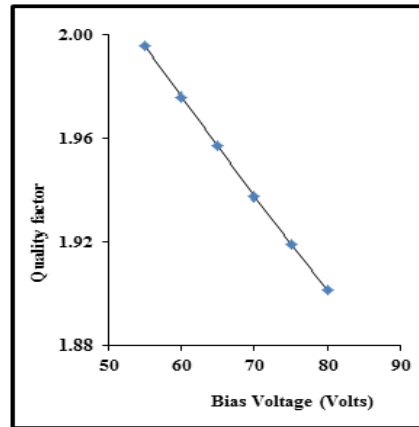


Fig.9: Variation of quality factor versus bias voltage for IMPATT diode loaded RMSA.

In order to compare IMPATT-loaded RMSA with unloaded patch only, calculations were made for various parameters which are shown graphically in Figures 10-16. From Fig.10, it is noted that the real part of impedance for both the cases decreases as frequency increases making the absolute value of impedance nearer to characteristic impedance of feed line of 50 ohms. However the reactive part of the impedance of unloaded patch decreases with the increases of resonant frequency (Fig.11).

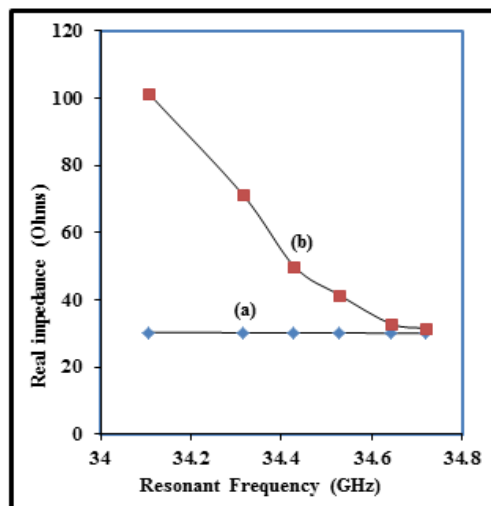


Fig.10: Variation of real impedance versus resonant frequency for (a) unloaded and (b) IMPATT diode

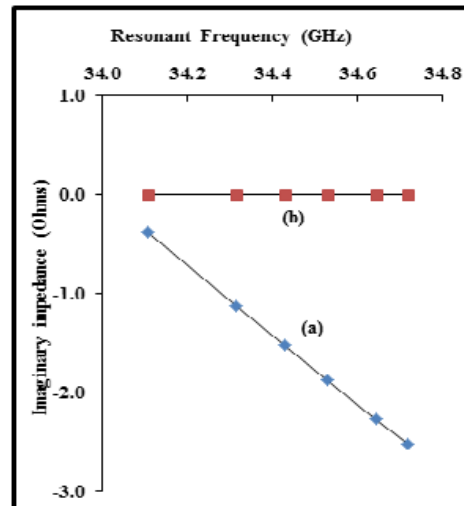


Fig.11: Variation of imaginary impedance versus resonant frequency for (a) unloaded and (b) IMPATT diode

It is observed that there is small variation in the real part of the impedance for unloaded patch with the bias voltage. The imaginary part of the impedance in unloaded patch is much lower than the inductive part of the impedance, showing that the unloaded patch antenna behaves as R-C network for the entire range of operation.

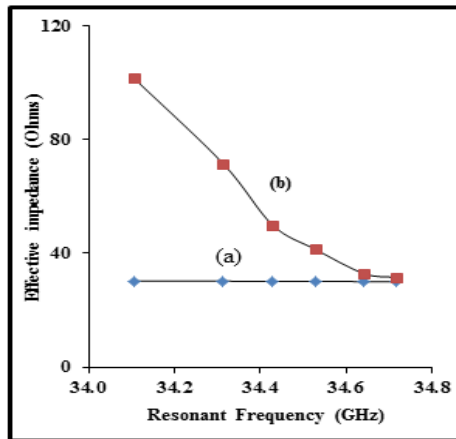


Fig.12: Variation of effective impedance versus resonant frequency for (a) unloaded and (b) IMPATT diode

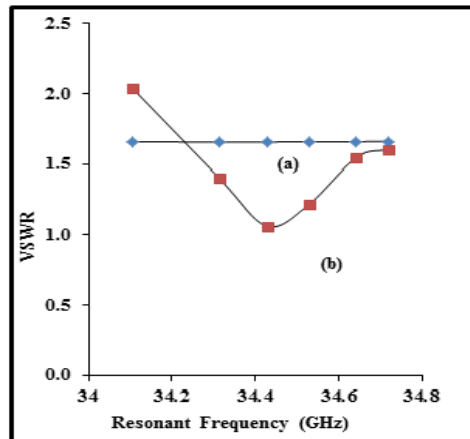


Fig.13: Variation of VSWR versus resonant frequency for (a) unloaded and (b) IMPATT diode loaded RMSA.

It may be further noted that the effective value of impedance is between 30.26 – 30.03 ohms for unloaded patch whereas it is 101.54 – 31.53 ohms(Fig.12) for loaded patch indicating that the integration of IMPATT diode makes the impedance of the patch quite high making the absolute impedance nearer to characteristic impedance of feed line of 50 ohms. These results can be further justified from the VSWR data, shown in Fig.13, which is lower as compared to unloaded patch, resulting in lower mismatch with the feed (Fig.14).

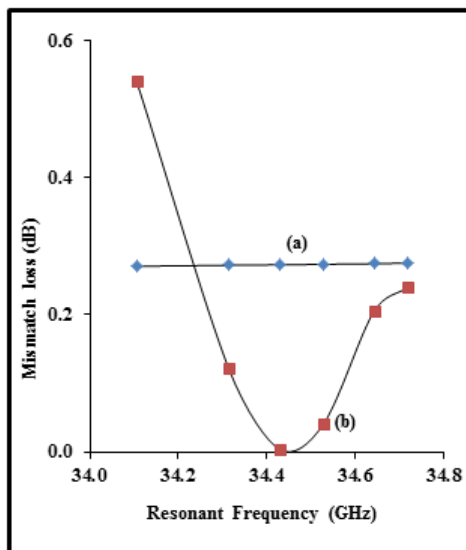


Fig.14: Variation of mismatch loss versus resonant frequency for (a) unloaded and (b) IMPATT diode loaded

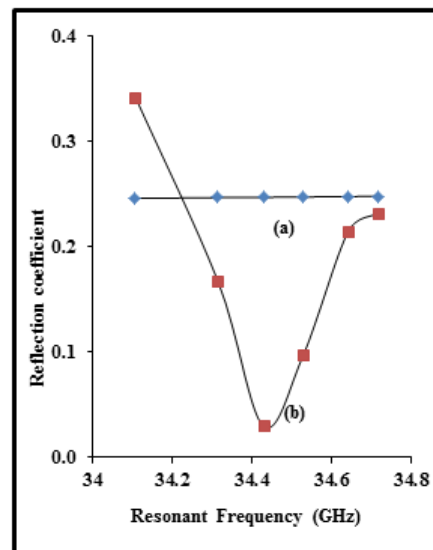
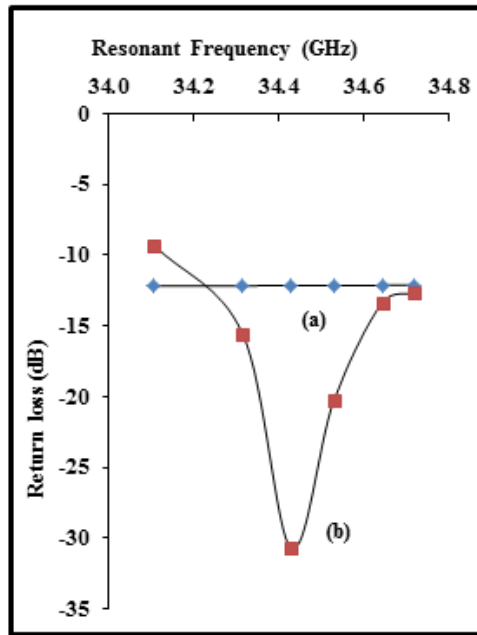


Fig.15: Variation of reflection coefficient versus resonant frequency for (a) unloaded and (b) IMPATT diode

These results are also corroborated from the results of reflection coefficient, return loss data shown in Figures 15-16. The examination of radiation pattern (Fig.17) of IMPATT loaded RMSA indicates that the E-plane radiated power is inversely proportional to the reverse bias voltage.



**Fig.16: Variation of return loss versus resonant frequency for (a) unloaded and (b) IMPATT diode loaded**

The radiation is maximum at higher reverse bias voltage. The radiated power decreases with decreasing bias voltage. The radiated power changes by 0.19 dB for the entire range of the bias voltage applied to the antenna for the obtainable tuning range 0.613.5 MHz thus providing power tunability in the considered active microstrip antenna. Hence IMPATT-loaded microstrip antenna is best suited for the power combining and active array applications.

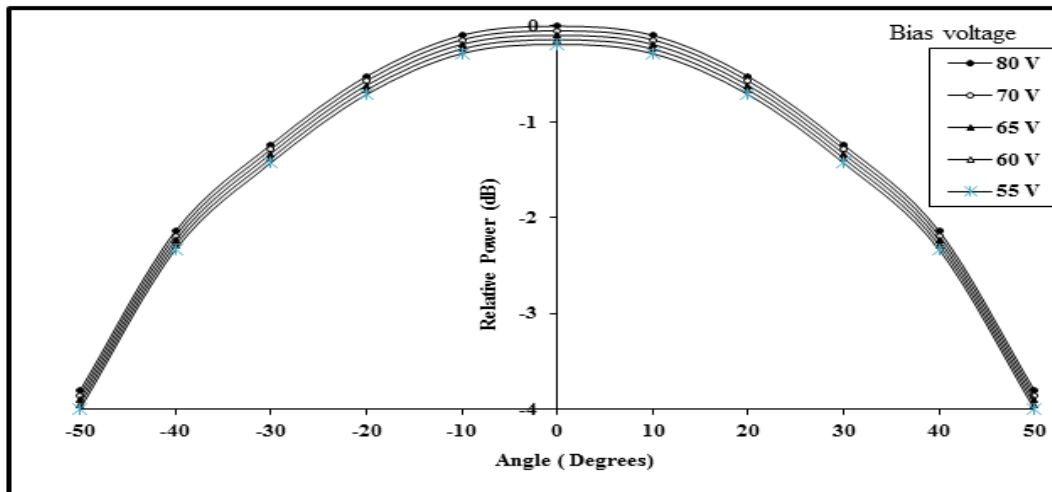


**Fig.17: Variation of E-plane radiated power with angle at different bias voltages for IMPATT loaded RMSA.**

## REFERENCES

- [1] Vinaybankey, N. Anvesh Kumar, Design and performance issues of Microstrip Antennas, International Journal of Scientific & Engineering Research, Volume 6(3), 2015



- [2] SanghamitraDasgupta and Bhaskar Gupta, Study and Analysis of GUNN Loaded Active Microstrip Patch Antenna, PIERS Proceedings, Kuala Lumpur, MALAYSIA, 27(30), 2012
- [3] Rakesh N. Tiwari, Prabhakar Singh, Tunnel Diode Loaded Microstrip Antenna with Parasitic Elements, Journal of Electromagnetic Analysis and Applications, Vol. 4, 2012
- [4] SomnathChatterjee, B. N. Biswas, Method for mounting Gunn Diode in Active Tapered Slot-Ring Antenna, Advanced Computational Techniques in Electromagnetics, Vol. 3, 2013
- [5] Anjali Nayak, V R Vishvakarma, IMPATT integrated active microstrip antenna; Indian Journal of Radio and Space Physics, Vol. 29(6), 2000
- [6] M V Schneider, Bell Sys. Technical Journal, 1960
- [7] D M Pozar, IEEE Trans. AP-30, 1982
- [8] S Y Lio, Microave Devices and Circuits (Prentice-Hall India, New Delhi 1992).
- [9] S M Sze; Microwave Devices and Circuits (John Wiley, New York 1969).
- [10] K R Carver and J W Mink, IEEE Trans. AP-29, 1981
- [11] H K Gummel and J L Blue; IEEE Trans, ED-14, 1967

**Table: 1**

**Typical parameters of IMPATT diode [11]**

Type	Si (N-type)
DC resistance (Z)	70 ohms
Oscillating frequency	(30 – 300) GHz
Operating mode	CW – mode
Passive resistance of inactive region	1.5 Ohms
Breakdown voltage ( $V_B$ )	94.1 V
DC reverse bias voltage (V)	(55 – 80) V
Diode cross-section area (A)	$10^{-8} \text{ m}^2$
Derivative of ionization coefficient with electric field ( $\alpha$ )	3.059
Carrier drift velocity ( $V_d$ )	$2 \times 10^5 \text{ m/sec}$
Semiconductor permittivity ( $\epsilon_s$ )	$1.0443 \times 10^{-11} \text{ F/m}$
Electric field	$4 \times 10^7 \text{ V/m}$



**Table: 2**

Rectangular patch specification[5]

Substrate material used	RT Duroid 5870
Relative dielectric constant ( $\epsilon_r$ )	2.32
Loss tangent (Tan $\delta$ )	0.0012
Thickness of substrate material (h)	1.524 mm
Width of patch (W)	3.42419 mm
Length of patch (l)	1.800792 mm
Resistance of the patch (R)	30.246 ohms
Inductance of the patch (L)	70.604 pH
Capacitance of the patch (C)	6.199 pF
Patch resistance at resonance ( $R_R$ )	157.94 Ohms
Diode radiation conductance ( $G_r$ )	0.00167 mho
Diode feed location ( $x_0$ )	1.22065 mm